Published by Institute of Physics Publishing for SISSA

Received: *October 4, 2007*
Revised: *November 8, 2007*
Accepted: *November 12, 2007*
Published: *November 27, 2007*

Holographic phase transitions at finite chemical potential

David Mateos,[a] **Shunji Matsuura,**[bc] **Robert C. Myers**[bd] **and Rowan M. Thomson**[bd]

[a] *Department of Physics, University of California, Santa Barbara, CA 93106-9530, U.S.A.*
[b] *Perimeter Institute for Theoretical Physics, Waterloo, Ontario N2L 2Y5, Canada*
[c] *Department of Physics, University of Tokyo, 7-3-1 Hongo, Bunkyoku, Tokyo, 113-0033, Japan*
[d] *Department of Physics and Astronomy, University of Waterloo, Waterloo, Ontario, N2L 3G1, Canada*
E-mail: dmateos@physics.ucsb.edu, smatsuura@perimeterinstitute.ca, rmyers@perimeterinstitute.ca, rthomson@perimeterinstitute.ca

Abstract: Recently, holographic techniques have been used to study the thermal properties of $\mathcal{N} = 2$ super-Yang-Mills theory, with gauge group SU(N_c) and coupled to $N_f \ll N_c$ flavours of fundamental matter, at large N_c and large 't Hooft coupling. Here we consider the phase diagram as a function of temperature and baryon chemical potential μ_b. For fixed $\mu_b < N_c M_q$ there is a line of first order thermal phase transitions separating a region with vanishing baryon density and one with nonzero density. For fixed $\mu_b > N_c M_q$ there is no phase transition as a function of the temperature and the baryon density is always nonzero. We also compare the present results for the grand canonical ensemble with those for canonical ensemble in which the baryon density is held fixed [1].

Keywords: Brane Dynamics in Gauge Theories, Gauge-gravity correspondence.

JHEP11(2007)085

Contents

1. Introduction

A large class of strongly coupled gauge theories can be studied using the gauge/gravity duality [2, 3]. In this context, the dynamics of a small number of flavours $N_{\rm f} \ll N_{\rm c}$ of fundamental matter in the gauge theory can be described by the dynamics of $N_{\rm f}$ D-branes in the appropriate dual geometry. At sufficiently high temperatures, for which the gauge theory is in a deconfined or plasma phase,[1] this geometry contains a black hole [4]. Since the condition $N_{\rm f} \ll N_{\rm c}$ ensures that the D-branes only perturb the background slightly, the dynamics of the fundamental matter in the deconfined phase corresponds to the dynamics of D-brane probes in a black hole background.

The thermal properties of $N_{\rm f}$ flavours of fundamental matter in SU($N_{\rm c}$) super-Yang-Mills (SYM) have been extensively studied using this holographic framework [5 – 9]. In these systems, the fundamental matter generically undergoes a first order phase transition at some critical temperature $T_{\rm fun}$. The low-temperature phase of the theory is described by 'Minkowski embeddings' of the probe branes (see figure 1) in which the branes sit entirely outside the black hole [6, 7]. In this phase, the meson spectrum is discrete and exhibits a mass gap. Above the critical temperature $T_{\rm fun}$, the branes fall through the horizon and the gravity system is characterised by these 'black hole' embeddings. In this phase, the meson spectrum is continuous and gapless [7, 10, 11]. Thus, this large-$N_{\rm c}$, strong coupling phase transition is associated with the melting or dissociation of mesons. As recently illustrated in related models [12], we emphasize that in theories that undergo a confinement/deconfinement phase transition at some temperature $T_{\rm dec} < T_{\rm fun}$, the phase transition for fundamental matter just described occurs as a separate phase transition. Instead, if $T_{\rm fun} < T_{\rm dec}$, both phase transitions take place simultaneously. In the former case, mesonic states remain bound for a range of temperatures $T_{\rm dec} < T < T_{\rm fun}$ despite the fact that the theory is in a deconfined phase.

This physics is in qualitative agreement with that of QCD. Studies from lattice QCD [13] suggest that some mesons survive the deconfinement phase transition at $T_{\rm dec} \sim$

[1] The theory may or may not undergo a phase transition to a confined phase at low temperatures.

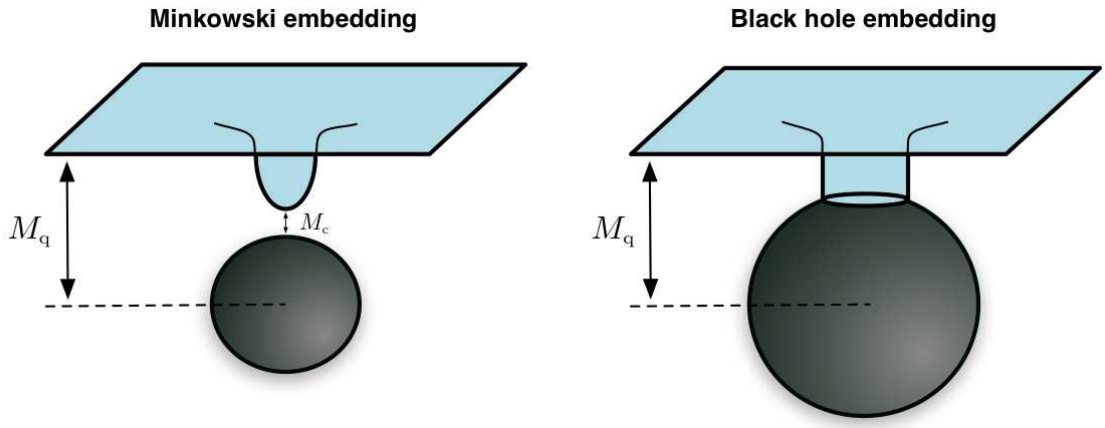

Figure 1: Possible D-brane embeddings in the black hole geometry.

175 MeV and remain as relatively well-defined resonances up to temperatures of $2-3\,T_{\rm dec}$. It is therefore interesting to consider how this physics is modified in the presence of a chemical potential $\mu_{\rm b}$ or nonzero density $n_{\rm b}$ for baryon number. In the holographic framework, the introduction of a chemical potential $\mu_{\rm b}$ or nonzero density $n_{\rm b}$ for baryon number corresponds to turning on the diagonal U(1) gauge field on the D-branes [1].

The phase diagram for the gauge theory at constant baryon number density $n_{\rm b}$ was studied in [1]. It was found that, for any nonzero value of the baryon number density $n_{\rm b}$, Minkowski embeddings are physically inconsistent. Simply stated, a nonzero density of baryons (or quarks) is dual to a worldvolume electric field, which in turn translates into a finite number of (fundamental) strings dissolved in the probe D-branes. Since the strings cannot simply terminate, it is not possible for the branes to close off smoothly above the horizon. Fortunately, for $n_{\rm b} \neq 0$ there exist black hole embeddings where the D-branes intersect the horizon for all values of the temperature. This is in contrast with the case $n_{\rm b} = 0$, in which black hole embeddings do not exist below a certain temperature and Minkowski embeddings are required to describe the system [6, 7]. Focussing on the D3/D7 system, i.e., $N_{\rm f}$ D7-brane probes in the black near-horizon geometry of $N_{\rm c}$ D3-branes, it was shown in ref. [1] that the physics is essentially continuous around $n_{\rm b} = 0$. For small $n_{\rm b}$, the black hole embeddings mimic the behaviour of both the Minkowski and black hole branches of the $n_{\rm b} = 0$ system, and a first order phase transition occurs between two different black hole embeddings – see ref. [1] for details. In a region with small $n_{\rm b}$, the $(T, n_{\rm b})$ phase diagram exhibits a line of thermal phase transitions which terminates at a critical point (at finite $n_{\rm b}$). However, it must be noted that the configurations below the phase transition were found to be unstable suggesting the existence of a new, perhaps inhomogeneous, phase. Though the focus in ref. [1] was on the D3/D7 system, general arguments presented there suggest that the same physics occurs in other Dp/Dq systems, corresponding to gauge theories in different dimensions [14].

JHEP11(2007)085

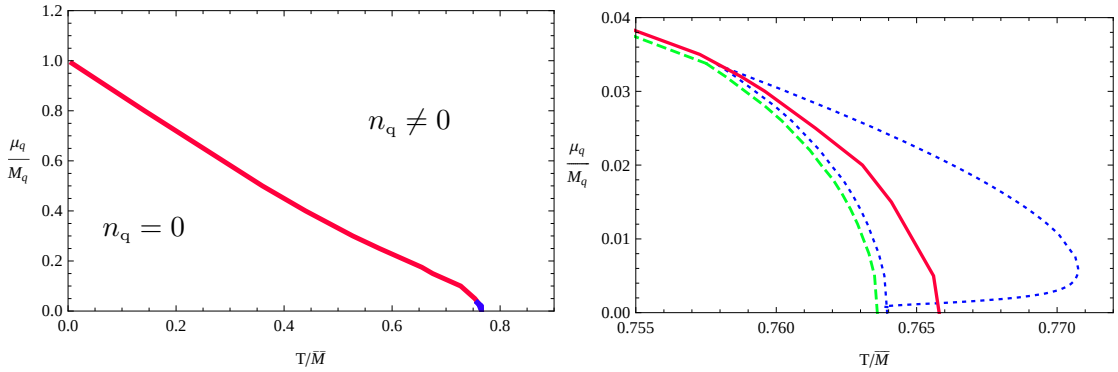

(a) (b)

Figure 2: Phase diagram: Quark chemical potential μ_q/M_q versus temperature $T/\bar{M}$. The red, continuous curve separates the phase of Minkowski embeddings (small temperatures, small μ_q/M_q) from black hole embeddings. Figure (b) zooms in on the region near the end of this line and also depicts the boundary of the region accessed by the black hole embeddings (green, dashed curve) and a small region (enclosed by the blue, dotted curve) where more than one black hole embedding is available for a given value of μ_q and T. The separation of the red and green curves would not be resolved on the scale of figure (a).

The above study of the thermodynamics with fixed n_b was performed in the canonical ensemble. Of course, the thermodynamics can also be studied in the grand canonical ensemble, in which the chemical potential μ_b is kept fixed. This is the focus of this paper. As described above and clearly elucidated in [1], the restriction to black hole embeddings only applies when n_b is fixed and nonvanishing. Hence, as we will describe, Minkowski embeddings play an essential role in describing the grand canonical ensemble. Again we consider only the D3/D7 brane system in the following but expect similar results for other Dp/Dq brane systems [14].

Our main result is the phase diagram displayed in figure 2, where

$$\mu_q = \frac{\mu_b}{N_c} \tag{1.1}$$

is the quark chemical potential and $\bar{M} \propto M_q$ is a mass scale defined in eq. (2.14) below. As we show in section 2, for fixed $\mu_q < M_q$ black hole embeddings do not exist below a certain temperature. In contrast, for $\mu_q > M_q$, black hole embeddings exist for all temperatures. On the other hand, Minkowski embeddings with a vanishing density of baryons, $n_b = 0$, exist for all μ_q up to a temperature $T \sim T_{fun}$. Our study in section 3 of the free energy of the system as the temperature increases reveals that for $\mu_q < M_q$ there is a first order phase transition from a Minkowski embedding to a black hole embedding. In the field theory this is a transition characterised by the condensation of charge, namely by a jump from a phase with $n_q = 0$ to a phase with $n_q \neq 0$. The meson spectrum across this transition also changes: In the low-temperature Minkowski phase the meson spectrum is discrete and possesses a mass gap, whereas in the high-temperature black hole phase it is continuous and gapless. For larger chemical potential, $\mu_q > M_q$, there is no phase transition as a function of the temperature.

JHEP11(2007)085

As described above, for $\mu_{\rm q} < M_{\rm q}$ black hole embeddings do not exist below a certain temperature. The boundary of the portion of the phase diagram accessed by these embeddings essentially coincides with the line of phase transitions shown in figure 2a. However, at higher resolution in figure 2b, one can see these two boundaries deviate in a small region near $\mu_{\rm q} \sim 0$. This figure also illustrates a small region of the phase diagram where more than one black hole embedding is available for a given value of $\mu_{\rm q}$ and T. In particular, the latter contains the black hole embeddings that are thermodynamically unstable. As will be discussed below, this 'multi-valued' region of black hole embeddings was central to the analysis of the phase transition studied in [1] for the canonical ensemble with fixed $n_{\rm q}$. In section 4, we discuss the reconciliation of these previous results with those found here.

While this paper was in the final stages of preparation, three related papers [15 – 17] appeared which have considerable overlap with our present investigation.

2. Holographic framework

Following [6, 7], the metric for $N_{\rm c}$ black D3-branes in the decoupling limit may be written as[2]

$$ds^2 = \frac{1}{2}\left(\frac{u_0\rho}{L}\right)^2\left[-\frac{f^2}{\tilde{f}}dt^2 + \tilde{f}d\vec{x}^2\right] + \frac{L^2}{\rho^2}\left[d\rho^2 + \rho^2 d\Omega_5^2\right] , \tag{2.1}$$

where ρ is a dimensionless coordinate and

$$f(\rho) = 1 - \frac{1}{\rho^4} , \quad \tilde{f}(\rho) = 1 + \frac{1}{\rho^4} , \quad L^4 = 4\pi g_{\rm s} N_{\rm c} \ell_{\rm s}^4 . \tag{2.2}$$

This metric possesses a horizon at $\rho = 1$ with temperature

$$T = \frac{u_0}{\pi L^2} , \tag{2.3}$$

which is identified with the temperature of the dual $\mathcal{N} = 4$ SYM theory. In turn, the coordinates $\{t, \vec{x}\}$ are identified with the coordinates of the gauge theory. The string coupling constant is related to the SYM 't Hooft coupling constant through

$$\lambda = g_{\rm YM}^2 N_{\rm c} = 2\pi g_{\rm s} N_{\rm c} . \tag{2.4}$$

In addition to the metric above, the D3-brane solution is characterised by a constant dilaton and a Ramond-Ramond field given by

$$C_{0123} = -\frac{(u_0\rho)^4 \tilde{f}^2}{4L^4} . \tag{2.5}$$

Introducing $N_{\rm f}$ D7-branes into the geometry above corresponds to coupling $N_{\rm f}$ fundamental hypermultiplets to the original SYM theory [18]. Before the decoupling limit, the branes are oriented as

$$\begin{array}{lcccccccccc} & 0 & 1 & 2 & 3 & 4 & 5 & 6 & 7 & 8 & 9 \\ \text{D3:} & \times & \times & \times & \times & & & & & & \\ \text{D7:} & \times & \times & \times & \times & \times & \times & \times & \times & & \end{array} \tag{2.6}$$

[2] This metric is related to the standard presentation through the coordinate transformation $(u_0\rho)^2 = u^2 + \sqrt{u^4 - u_0^4}$.

This configuration is supersymmetric at zero temperature, which ensures the stability of the system. After the decoupling limit, the D7 branes wrap an S^3 of possibly varying radius inside the S^5 of the background geometry. Writing

$$d\Omega_5^2 = d\theta^2 + \sin^2\theta d\Omega_3^2 + \cos^2\theta d\phi^2 \tag{2.7}$$

and defining $\chi = \cos\theta$, the embedding of the D7-branes is described by $\phi = 0$, $\chi = \chi(\rho)$.

As discussed in detail in ref. [1], in order to study the gauge theory at finite chemical potential or baryon number density, it suffices to consider a radial electric field on the D7-branes. Choosing the gauge $A_\rho = 0$, this can be described by a gauge field time component of the form $A_t(\rho)$. The derivation of the equations of motion for $\chi(\rho)$ and $A_t(\rho)$ was discussed in [1] and we review a few salient details here.

The (Dirac-Born-Infeld) action of the D7-branes is

$$I_{\rm D7} = -N_{\rm f} T_{\rm D7} \int dt\, d^3x\, d\rho\, d\Omega_3 \frac{(u_0\rho)^3}{4} f\tilde{f}(1-\chi^2)\sqrt{1-\chi^2+\rho^2\dot{\chi}^2 - \frac{2\tilde{f}}{f^2}(1-\chi^2)\dot{\tilde{A}}_t^2}\,, \tag{2.8}$$

where the dot denotes differentiation with respect to ρ and we have introduced a dimensionless gauge field

$$\tilde{A}_t = \frac{2\pi\ell_{\rm s}^2}{u_0} A_t\,. \tag{2.9}$$

Note that $\dot{\tilde{A}}_t$ corresponds to a radial electric field. The corresponding equation of motion (eq. (2.11) in [1]) dictates that asymptotically

$$A_t = \mu_{\rm q} - \frac{u_0}{2\pi\ell_{\rm s}^2}\frac{\tilde{d}}{\rho^2} + \cdots\,, \tag{2.10}$$

where the constant $\mu_{\rm q}$ is the quark chemical potential and $\tilde{d}$ is a dimensionless constant related to the vacuum expectation value of the quark number density operator through

$$n_{\rm q} = \frac{1}{2^{5/2}} N_{\rm f} N_{\rm c} \sqrt{\lambda}\, T^3\, \tilde{d}\,. \tag{2.11}$$

The equation of motion for χ (eq. (2.17) in [1]) implies that the branes' profile behaves asymptotically as

$$\chi = \frac{m}{\rho} + \frac{c}{\rho^3} + \cdots\,, \tag{2.12}$$

where the dimensionless constants m and c are proportional to the quark mass and condensate, respectively [6, 7]. In particular

$$m = \frac{\bar{M}}{T}\,, \tag{2.13}$$

where the scale

$$\bar{M} = \frac{2M_{\rm q}}{\sqrt{\lambda}} = \frac{M_{\rm gap}}{2\pi} \tag{2.14}$$

is (up to a factor) the meson mass gap $M_{\rm gap}$ in the D3/D7 brane theory at zero temperature [21].

JHEP11(2007)085

Let us now consider what types of embeddings are possible if $\mu_q \neq 0$. As shown in [6, 7], Minkowski embeddings only exist for $T/\bar{M} \lesssim 0.77$, i.e., for sufficiently low temperatures or sufficiently large quark masses. Moreover, these embeddings are physically consistent only if $n_q = 0$ [1]. However, the chemical potential can take any value, since a Minkowski embedding with $A_t = \mu_q$ is a solution of the equations of motion if the same embedding is a solution with $A_t = 0$.[3] Thus Minkowski embeddings describe a phase with a possibly nonzero chemical potential but vanishing charge density. We therefore expect (and we will confirm below) that these embeddings are thermodynamically preferred if $\mu_q \lesssim M_c$, where M_c is the constituent or thermal quark mass at a given temperature. As shown in figure 1, this mass is proportional to the distance between the tip of the D7-branes and the horizon, in contrast to the bare quark mass M_q, which is proportional to the asymptotic distance between the D7-branes and the D3-branes [7, 19].

If $n_q \neq 0$ then only black hole embeddings are physically consistent, and these exist for all values of $T/\bar{M}$. Regularity requires the gauge field to vanish at the horizon,[4] so the chemical potential can be expressed in terms of $\tilde{d}$, T and M_q by integrating Gauss' law from the horizon to the boundary as [1]

$$\mu_q = \frac{u_0}{2\pi\ell_s^2}\, 2\tilde{d} \int_1^\infty d\rho\, \frac{f\sqrt{1-\chi^2+\rho^2\dot{\chi}^2}}{\sqrt{\tilde{f}(1-\chi^2)\left[\rho^6\tilde{f}^3(1-\chi^2)^3+8\tilde{d}^2\right]}}\,. \tag{2.15}$$

A key observation now is the fact that, for sufficiently small $T/\bar{M}$, μ_q approaches a nonzero value in the limit $n_q \to 0$. This is illustrated in figure 3, which displays μ_q/M_q as a function of $T/\bar{M}$ for decreasing values of $\tilde{d}$ (from top curve to bottom curve) all the way down to $\tilde{d} = 10^{-4}$. Taking $\tilde{d}$ to be even smaller than this value does not yield values of μ_q appreciably smaller on the scale shown in the figure. In other words, black hole embeddings only cover the region above the bottom curve in figure 3. This observation is important because it means that Minkowski embeddings are necessary to describe the region below this curve.

The curves in figure 3 were obtained by numerical integration of eq. (2.15). However, analytic results can be obtained in the limiting cases of large and small $T/\bar{M}$. In the limit $T/\bar{M} \to 0$ with fixed $\tilde{d}$, it was shown in [1] that $\mu_q \to M_q$ regardless of the value of $\tilde{d}$. This is reflected in figure 3 by the fact that all curves meet on the vertical axis at $\mu_q/M_q = 1$. In the opposite limit, $\bar{M}/T \to 0$, the embedding becomes simply $\chi(\rho) = 0$. Substituting this into (2.15) one obtains an expression that can be easily integrated. In particular, one

[3] Note that these two solutions are not gauge-equivalent, since they differ in the non-normalizable mode of the gauge field. Gauge transformations that are proper symmetries of the theory must tend to the identity at asymptotic infinity, and hence cannot change the non-normalisable mode of the gauge field.

[4] To see this, note that the event horizon of the background (2.1) can be characterised as a Killing horizon, which implies that it contains the bifurcation surface. The latter is a fixed point of the Killing flow where the corresponding Killing vector vanishes, i.e., $\partial_t = 0$ on the bifurcation surface, as opposed to the null condition $|\partial_t|^2 = 0$ which is also realized elsewhere on the horizon [20]. Hence if the potential A as a one-form is to be well defined, then A_t must vanish there. This is, of course, the Lorentzian analog of the topological constraint which arises more intuitively for the corresponding Euclidean black hole.

JHEP11(2007)085

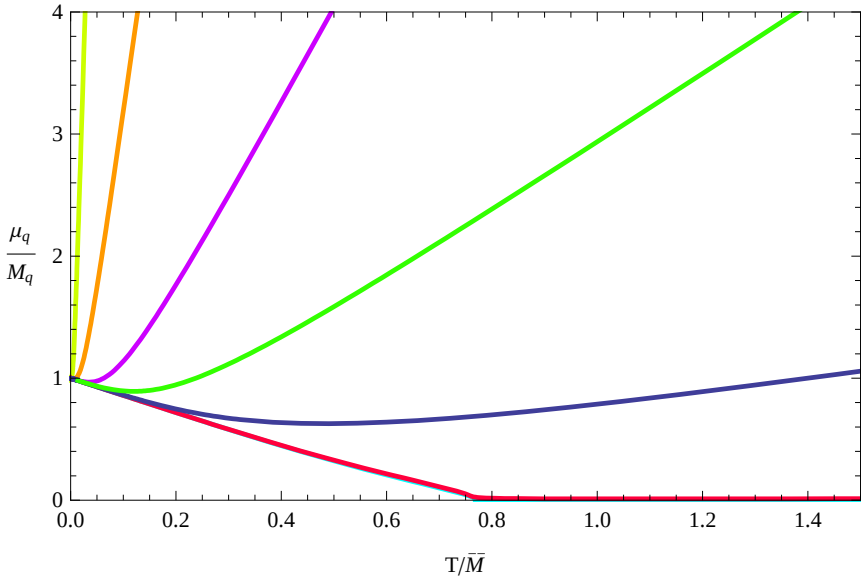

Figure 3: Chemical potential $\mu_{\rm q}/M_{\rm q}$ versus $T/\bar{M}$ for various values of $\tilde{d}$, increasing from bottom up: $\tilde{d} = 10^{-4}$, 10^{-2}, 1, 10, 104, 4298, 380315. The $\tilde{d} = 10^{-4}$, 10^{-2} lines are virtually coincident.

easily verifies in this case that

$$\mu_{\rm q} \simeq \frac{u_0\,\tilde{d}}{4\pi\ell_{\rm s}^2} + O(\tilde{d}^3) = \frac{2}{N_{\rm f}\,N_{\rm c}}\,\frac{n_q}{T^2} + O(n_q^3) \tag{2.16}$$

for small $\tilde{d}$, and consequently $\mu_{\rm q} \to 0$ as $\tilde{d} \to 0$.

To summarise, we conclude that the region of small $\mu_{\rm q}/M_{\rm q}$ and small $T/\bar{M}$ (the triangular region below the bottom line in the lower left corner of figure 3) must be described by Minkowski embeddings. Similarly, the region with $T/\bar{M} \gtrsim 0.77$ must be described by black hole embeddings. In order to decide what the favoured embedding is in the rest of the parameter space, i.e., in the region in which both Minkowski and black hole embeddings exist, we must determine which embedding minimises the free energy of the system.

3. Thermodynamics

From the previous section it is clear that both Minkowski and black hole embeddings play a role in the grand canonical ensemble. As both embeddings exist for certain values of temperature and chemical potential, it is necessary to study the thermodynamics to determine the physically preferred configuration. To this end, we use the standard technique of Wick rotating [22] the time direction. Then, the leading contribution to the free energy is determined by evaluating the Euclidean action. As we are interested in the behaviour of the fundamental matter, we only consider the action for the D7-branes.

Of course, the Euclidean action for the D7-branes is given by Wick-rotating the action in (2.8). Evaluating this action leads to a formally divergent result. However, the divergences are removed by introducing a finite-radius ultraviolet cut-off and a set of boundary

JHEP11(2007)085

counterterms to renormalise the action [24]. This holographic renormalisation was discussed in detail in [1, 6, 7] and the result, from ref. [1], is

$$\frac{I_{\rm E}}{\mathcal{N}} = G(m) - \frac{1}{4}\left[(\rho_{\rm min}^2 - m^2)^2 - 4mc\right] , \tag{3.1}$$

where $G(m)$ is the convergent integral[5]

$$G(m) = \int_{\rho_{\rm min}}^{\infty} d\rho \left(\rho^3 f \tilde{f}(1-\chi^2)\sqrt{1-\chi^2+\rho^2\dot{\chi}^2 - \frac{2\tilde{f}}{f^2}(1-\chi^2)\dot{\tilde{A}}_t^2} - \rho^3 + m^2\rho \right) , \tag{3.2}$$

$\mathcal{N}$ is a normalisation constant given by

$$\mathcal{N} = \frac{1}{32}\lambda N_{\rm f} N_{\rm c} T^3 , \tag{3.3}$$

and $\rho_{\rm min}$ is the minimum value of ρ for the embedding of interest.

This Euclidean action of the D7-branes is identified with their Gibbs free energy $W(T, \mu_{\rm q})$ via $W = T I_{\rm E}$ [1]. Of course, the thermodynamically preferred D7-brane embedding is that which minimises the free energy and hence we evaluated the free energy as a function of temperature for fixed $\mu_{\rm q}/M_{\rm q}$. Representative plots of the free energy (scaled by $\bar{\mathcal{N}} = \lambda N_{\rm f} N_{\rm c} \bar{M}^4/32$) versus temperature are provided in figures 4 and 5. The results for $\mu_{\rm q}/M_{\rm q} = 0.0108$ (figure 4) are typical for small $\mu_{\rm q}/M_{\rm q}$, displaying the classic 'swallow tail' shape and closely resembling the $\mu_{\rm q} = 0$ results (shown in figure 5 of [7]). For larger $\mu_{\rm q}/M_{\rm q}$, the 'swallow tail' shape disappears — see figure 5. For $\mu_{\rm q}/M_{\rm q} < 1$, the two branches still cross at some temperature and this, of course, determines the temperature of the phase transition — see figure 5a. As $\mu_{\rm q}/M_{\rm q}$ increases towards 1, the temperature of the phase transition decreases. The results in figure 5b are typical for large $\mu_{\rm q}/M_{\rm q}$: The two branches never cross and the free energy is always lower on the black hole branch.

By varying $\mu_{\rm q}/M_{\rm q}$ and examining the free energy, the phase diagram in figure 2 was mapped out. For $\mu_{\rm q}/M_{\rm q} < 1$, there is a phase transition corresponding to a discontinous jump from a Minkowski to a black hole embedding. As $\mu_{\rm q}/M_{\rm q}$ increases towards one, the temperature of the phase transition decreases. For larger chemical potentials, $\mu_{\rm q}/M_{\rm q} > 1$, there is no phase transition, with black hole embeddings thermodynamically favoured for all temperatures. Other thermodynamic quantities can be computed from the free energy, e.g., the entropy $S = (\partial W/\partial T)_{\mu_{\rm q}}$. Discontinuities in thermodynamic quantities (e.g., quark condensate, entropy density) at the phase transition indicate that the phase transition is first order. As illustrated in figure 5, however, the size of the discontinuity is becoming smaller and smaller as we approach $\mu_{\rm q}/M_{\rm q} = 1$. In fact, recent analytic work [17] indicates that this is a critical point where the phase transition becomes second order. For $\mu_{\rm q}/M_{\rm q} < 1$, the low temperature phase is described by Minkowski embeddings and hence $n_{\rm q} = 0$ below the phase transition. After the phase transition, $n_{\rm q} > 0$ and it increases

[5]For simplicity, we have left A_t untouched here rather than introducing a Wick rotated potential $A_{t_{\rm E}} = -i\,A_t$. As is well-known, such a Euclidean potential would have to be treated as an imaginary field in the present context because the chemical potential and particle density must remain real constants — see, e.g., [25].

JHEP11(2007)085

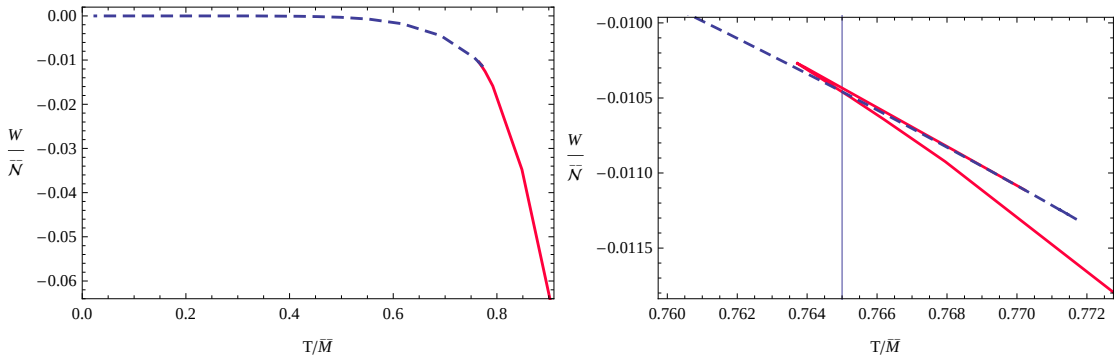

Figure 4: Free energy versus temperature for $\mu_q/M_q = 0.0108187$. The blue dotted line (red solid) represents the Minkowski (black hole) branch. The vertical line marks the temperature of the phase transition.

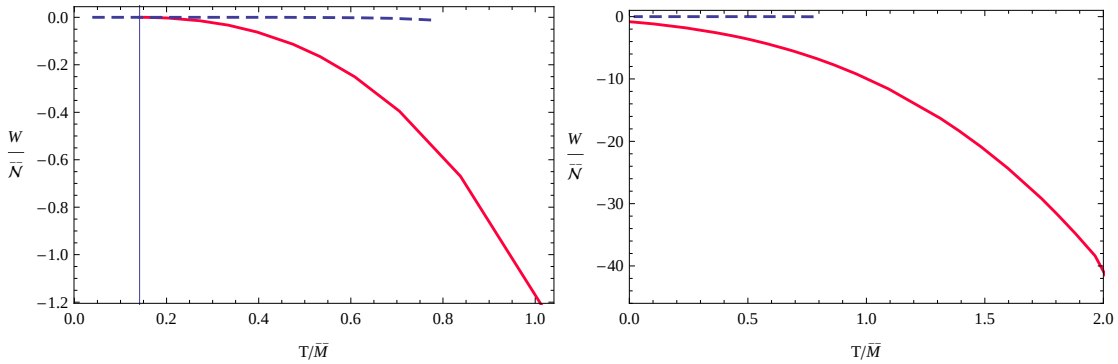

(a) $\mu_q/M_q = 0.8$ (b) $\mu_q/M_q = 2$

Figure 5: Free energy versus temperature for (a) $\mu_q/M_q = 0.8$ and (b) $\mu_q/M_q = 2$. In (a), the vertical line marks the temperature of the phase transition.

as the temperature increases. Similarly, for $\mu_q/M_q > 1$, n_q increases as the temperature increases.

Finally, we turn briefly to the thermodynamic stability of the system. The conditions for stability can be stated in different ways. Generally they can be phrased as the restriction that the Hessian of the state function, here the Gibbs free energy, is positive semi-definite. A simpler approach is to examine the necessary (but not sufficient) conditions:

$$\left.\frac{\partial S}{\partial T}\right|_{\mu_q} > 0\,, \quad \left.\frac{\partial n_q}{\partial \mu_q}\right|_{T} > 0\,, \tag{3.4}$$

which ensure that the grand canonical ensemble is stable against fluctuations purely in energy or charge. In ref. [1], it was stated that in the canonical ensemble the first requirement with fixed n_q (rather than fixed μ_q) appears to be satisfied everywhere, however, more recently ref. [15] reported that there are some regimes where the latter condition fails to hold. At present, we have found no indications that the grand canonical ensemble suffers such an energetic instability. Further, ref. [1] found that the second condition does not hold for some black hole embeddings.

JHEP11(2007)085

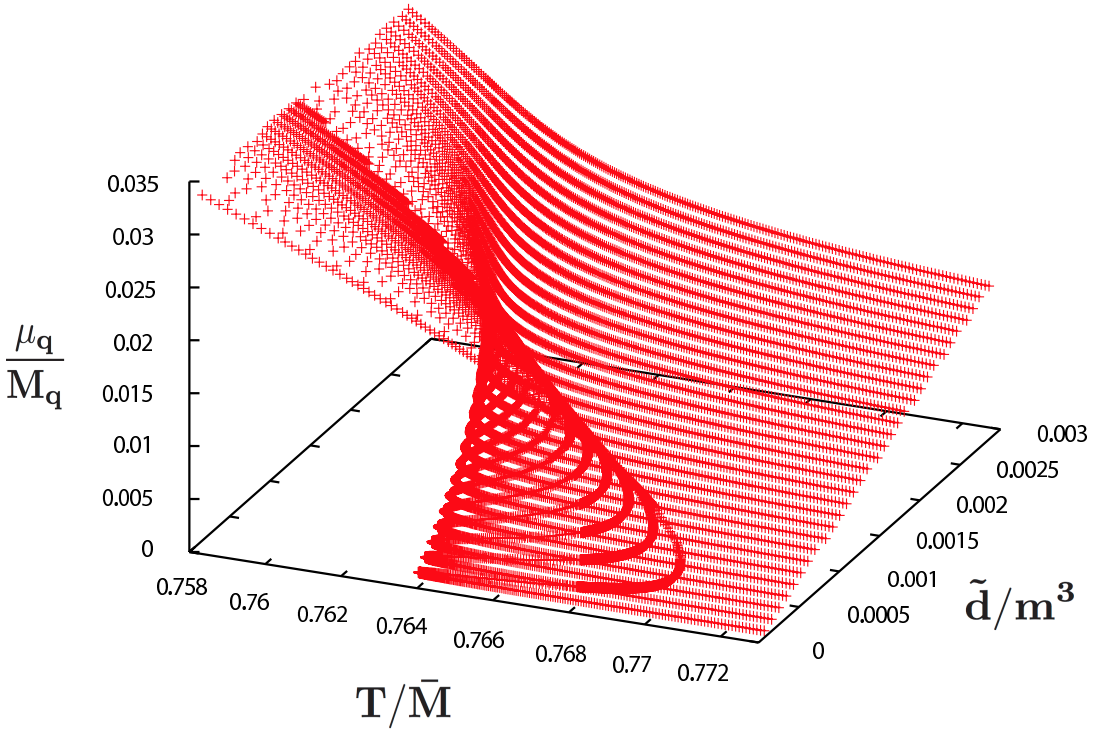

Figure 6: Three-dimensional plot of the chemical potential, the temperature and the charge density determined by black hole embeddings.

These unstable configurations can be found by examining figure 6, which illustrates μ_q as a function of T and n_q for the black hole embeddings — note that $\tilde{d}/m^3 \propto n_q/M_q^3$ is independent of T. The figure only covers a small region near the phase transition found in the canonical ensemble. In this regime, the surface $\mu_q(T, n_q)$ displays an interesting 'fold' and in the phase transition described in [1], the system jumps between configurations on the top and bottom of this fold. One can see that the unstable configurations discussed above correspond to the top of the fold illustrated in figure 6. These unstable embeddings then play a central role in the phase transition found for the canonical ensemble. In figure 2, these unstable configurations appear near the top of the multi-valued region enclosed by the blue curve and hence they could in principle play a role in this regime for the grand canonical ensemble as well. However, it turns out that minimizing the Gibbs free energy always picks out either a stable black hole or Minkowski embedding in this regime. Hence the system never suffers from this electrical instability. This result poses an apparent paradox though since (in the infinite volume limit, as applies here) the canonical and grand canonical ensembles should be equivalent [23], whereas here they seem to display different behaviours. We address this issue in the discussion below.

4. Discussion

A universal, first order, thermal phase transition in Dp/Dq systems was identified in [6], characterised by a jump of the Dq-branes from a Minkowski to a black hole embedding

JHEP11(2007)085

in the Dp-brane geometry. In the dual gauge theory, the transition is associated with the melting or dissociation of mesons. The analysis of ref. [6] was extended to include a nonzero quark density in ref. [1], where it was found that Minkowski embeddings are physically inconsistent for any $n_{\rm q} \neq 0$. Despite this, a first order thermal phase transition, in this case between two black hole embeddings, was found to occur for densities below a certain critical density.

In this paper we have examined the thermal behaviour of the D3/D7 system as a function of the quark chemical potential $\mu_{\rm q}$, as opposed to the quark density $n_{\rm q}$. As described in the introduction and clearly elucidated in [1], the restriction to black hole embeddings only applies when $n_{\rm q}$ is fixed and nonvanishing[6] and so no longer applies in describing the grand canonical ensemble. In particular then, we have found that, for $\mu_{\rm q} < M_{\rm q}$, the low-temperature phase is described by Minkowski embeddings with $n_{\rm q} = 0$. If the temperature is kept fixed and the chemical potential is increased to a critical value, or viceversa, the system undergoes a first order phase transition characterised by a jump to a black hole embedding with $n_{\rm q} \neq 0$. Thus the phase transition is characterised by the condensation of charge. The meson spectrum for the low-temperature phase was calculated in ref. [7] and is discrete and exhibits a mass gap. In the high-temperature phase there are no stable mesons and we expect a discrete spectrum of quasinormal modes [10, 11]. Hence, as with the $\mu_{\rm q} = 0$ case [6, 7], a dramatic feature characterising the phase transition is the melting of mesons. Unlike in the $\mu_{\rm q} = 0$ case, however, there is a finite density of quarks in the high-temperature phase, and this density increases with temperature. Figure 2a shows that the temperature of the phase transition decreases as $\mu_{\rm q}/M_{\rm q}$ increases towards one.

For $\mu_{\rm q} > M_{\rm q}$, there is no phase transition: In the gravity system, there are black hole embeddings of the D7-branes corresponding to all temperatures. Computing the free energy of these configurations and comparing to the results for the Minkowski embeddings reveals that the black hole embeddings are thermodynamically preferred. It would be interesting to examine the effect of a nonzero chemical potential on the transport properties of the D3/D7 plasma in this regime by extending the analysis of refs. [8, 10, 26, 27].

In this black hole phase we expect the meson spectrum to be continuous and gapless. The true quasi-particle excitations of the system, if any, correspond to 'quasinormal modes' of the D7-brane worldvolume fields [11]. In a regime in which the imaginary part of the quasinormal frequency is small, these excitations can be interpreted as quasi-particles in the dual quark-gluon plasma. Such long-lived quasi-particle excitations yield particularly striking resonances in the corresponding spectral functions. Such resonances were found for the D3/D7-brane system with $n_q = 0$ in [10, 27] but these were most pronounced for unstable black hole embeddings. Hence, it would be particularly interesting to study the spectrum of quasinormal modes [10, 11] or spectral functions [10, 27] in detail in the present context since, as described in [1], we expect to find a class of almost stable meson excitations in the regime of low temperature and low quark density where the black hole embeddings should be stable.

[6]Refs. [15, 28] attempt to construct Minkowski embeddings with $n_{\rm q} \neq 0$ but we believe these are unphysical for the reasons described in [1].

JHEP11(2007)085

Let us expand on this point: In this regime of low temperature and low quark density, the D7-brane connects to the event horizon with a long narrow spike. This black hole embedding then mimics the behaviour of a Minkowski embedding with (a gas of) fundamental strings stretching down to the horizon [1]. Hence the quasinormal spectrum should include long-lived modes that mimic the spectrum of (stable) mesons on the corresponding Minkowski embedding. It is relevant here to recall that the Minkowski phase also contains stable unconfined quarks described by strings stretched between the brane and the horizon. We note that these quarks also have unstable excited states described by the quasinormal modes on the strings. Presumably the quasinormal spectrum of the black hole embedding must also include modes which mimic this behaviour. On the black hole embedding, these modes describing 'quark excitations' would have support primarily on the spike connected to the horizon, in contrast to the 'mesonic' modes whose support would be primarily above the spike. Given the standard intuition for holographic energy scales [29], one may expect $T < \mathrm{Re}(\omega) < M_{\mathrm{q}}/\sqrt{\lambda}$ for the 'quark excitations'. In contrast, the imaginary part of the longest-lived modes is of order $\mathrm{Im}(\omega) \sim \sqrt{\lambda}T^2/M_{\mathrm{q}} \ll T$ in the regime considered here [19]. Hence it is possible that these modes may represent an independent class of quasiparticle excitations in the quark-gluon plasma.

In the Minkowski phase the spectrum contains mesons and quarks, and both sets of excitations are absolutely stable in the large-N_{c}, large-λ approximation considered here. In view of the presence in the spectrum of stable, quark-number-carrying states, it may seem surprising that the physics in the Minkowski phase is completely independent of μ_{q}, in particular that the quark density vanishes in this phase. After all, at finite temperature one expects a gas of quarks and anti-quarks to be present, and thus a finite chemical potential to induce a charge imbalance. The resolution of this puzzle comes from the fact that the quark mass is of order M_{q}, whereas the maximum temperature for which Minkowski embeddings are thermodynamically preferred is set by the meson mass and is therefore parametrically smaller: $T \sim T_{\mathrm{fun}} \sim M_{\mathrm{q}}/\sqrt{\lambda}$. Thus the abundance of quarks and anti-quarks in the thermal gas is proportional to the Boltzman factor

$$e^{-M_{\mathrm{q}}/T} \simeq e^{-\sqrt{\lambda}}. \tag{4.1}$$

This is exponentially suppressed at strong coupling, and hence is presumably invisible on the gravity side at leading order in the large-λ, large-N_{c} approximation under consideration.

One may also wonder whether baryons may play a role in the Minkowski phase. From the gauge theory viewpoint, we do not expect this to be the case, since the baryon mass scales as N_{c} and hence the baryon abundance at finite temperature is suppressed by $\exp(-N_{\mathrm{c}})$. On the gravity side, at strictly zero temperature, stable baryons are represented by D5-branes wrapping the S^5 part of the geometry [30] and connected to the D7-branes to induce an electric flux corresponding to N_{c} fundamental strings [21]. However, our intuition is that upon introducing a nonzero temperature, the gravitational attraction of the black hole causes the D5-branes to collapse and they are pulled behind the event horizon leaving behind just a black hole embedding of the D7-branes. We have performed some numerical investigations that seem to support this conclusion, but our results remain preliminary.

JHEP11(2007)085

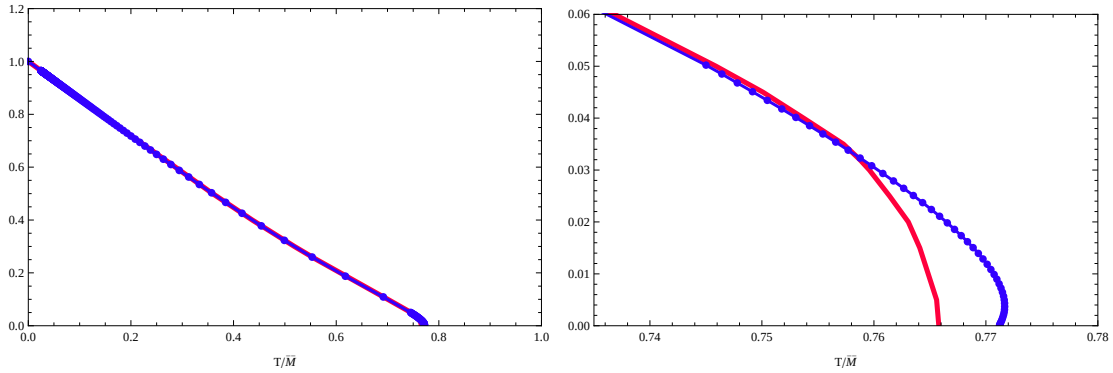

(a) (b)

Figure 7: Comparison of the ratio M_c/M_q (blue, dotted curve) with the ratio μ_q/M_q (red, continuous curve) at which the phase transition from a Minkowski to a black hole embedding takes place. The two curves essentially coincide on the scale of the figure (a).

Specifically, we have investigated the possible existence of tear-drop configurations,[7] similar to those of [31].[8] These configurations would end on a cusp above the horizon that could be connected to a cuspy D7-brane configuration along a number of fundamental strings. The tension of the strings would then overcome the tension of the branes [1] and presumably force the D5-branes and the D7-branes to connect to each other, resulting in a smooth configuration. However, our preliminary results indicate that there are no static configurations of this type. It is interesting to imagine a dual description of the dynamical collapse of the suggested tear-drop configurations. One would begin with a baryon as an excited state of bound quarks which are then dispersed as free quarks by the thermal bath of the strongly coupled gauge theory. In any event, we re-iterate that our numerical investigations here are only preliminary.

In the limit $T \to 0$ or $M_q \to \infty$, the phase transition from a Minkowski to a black hole embedding happens exactly at $\mu_q = M_q$. One can see this as arising from the fact that the D3/D7 system is supersymmetric at $T = 0$. In this limit the force exerted on the D7-branes by the background sourced by the D3-branes vanishes and the D7-branes are not deformed [21]. This implies that the constituent quark mass exactly coincides with the bare quark mass, $M_c = M_q$. It is therefore not surprising that the phase transition takes place when the chemical potential reaches this mass. The constituent quark mass for $T > 0$ (on Minkowski embeddings with $n_q = 0$) was calculated in [7, 19]. Figure 7 shows the ratio M_c/M_q (blue, dotted curve) as a function of temperature, as well as the value of the ratio μ_q/M_q (red, continuous curve) at which the phase transition takes place. It is

[7] One might also consider cone-like configurations in which the D5-brane has already partially fallen through the event horizon. These would describe a mixed phase of baryons and unbound quarks, if they were stable, but our intuition is that they are also unstable.

[8] Note that the D5-brane configurations studied in [31] do not correspond to baryons in the four-dimensional $\mathcal{N} = 4$ SYM theory at finite temperature. The gravitational background in [31] corresponds to the AdS soliton rather than an AdS black hole, so the baryons considered in that reference are baryons in a confining phase of the gauge theory produced by compactifying one of the dimensions.

JHEP11(2007)085

remarkable that the two curves are almost coincident except for relatively small values of $\mu_{\rm q}$, i.e., towards the higher temperature end of the line of phase transitions. A similar result was found recently in [16] for a similar holographic gauge theory. We note that the two curves in figure 7b begin to diverge significantly at $T \simeq .758\bar{M}$, which coincides with the temperature where the line of phase transitions enters the multi-valued region in figure 2b. This agreement seems better than one is in principle entitled to expect. That is, figure 7 illustrates that the chemical potential required to introduce quarks into the gluon plasma essentially matches the energy of a 'free' quark. We have put 'free' in quotes because the constituent quark mass $M_{\rm c}$ does take into account the interactions of an individual quark with the strongly coupled plasma of adjoint fields. However, the agreement in figure 7 then indicates that the interactions between the quarks themselves are largely negligible at the phase transition.

This result may further suggest that the density of quarks should be small just above the phase transition. Examining figure 8, we see that this statement seems to be correct in that the dimensionless ratio $r = \tilde{d}/m^3$ is indeed much less than one. Further we note that r is largest towards the higher temperature end of the line of phase transitions, i.e., roughly in the same region where the two curves in figure 7b deviate from one another. However, using eqs. (2.11)–(2.14), we find

$$n_{\rm q} = \sqrt{2}\, r\, \lambda N_{\rm f} N_{\rm c}\, n_{\rm crit} \qquad \text{with} \quad n_{\rm crit} \equiv \left(\frac{M_{\rm q}}{\sqrt{\lambda}}\right)^3 . \tag{4.2}$$

Above we have defined $n_{\rm crit}$ keeping in mind that studies of structure functions [32], as well as mapping of a quark's disturbance of the adjoint fields [33], both indicate that the size of (the glue cloud around) an individual quark is roughly $(M_{\rm q}/\sqrt{\lambda})^{-1}$ (at $T = 0$). Hence we might expect that the quarks would begin to interact significantly when the quark density reaches $n_{\rm crit}$. Therefore, even though r may be of the order .0001 (as at the phase transition in figure 8), eq. (4.2) indicates that $n_{\rm q} \gg n_{\rm crit}$ because we are in the limit of large λ and large $N_{\rm c}$. Hence the good agreement between $\mu_{\rm q}$ and $M_{\rm c}$ suggests the surprising result that the quark-quark interactions have a negligible effect even at parametrically large quark densities.

Let us comment on the supergravity description of these results. The constituent quark mass is defined as the energy of a test fundamental string stretching between the tip of the D7-branes and the horizon [7, 19]. In the absence of supersymmetry (i.e., at $T > 0$), this energy need not coincide with the energy of a 'spike' emanating from the D7-branes down to the horizon. This spike in the D7-brane geometry extends uniformly in all of the gauge theory directions. Hence this spike accounts for the effects of the interactions of the quarks with both adjoint fields and other quarks. In other words, this geometry, which represents the presence of a macroscopic string density, has an energy which receives contributions not accounted for by the test string calculation, such as (for example) the deformation of the D7-branes.

Before closing we would like to comment on the relation between the present results and those presented in [1]. There for the canonical ensemble with fixed $n_{\rm q}$, we found a first order phase transition that only existed for small charge densities and temperatures near

JHEP11(2007)085

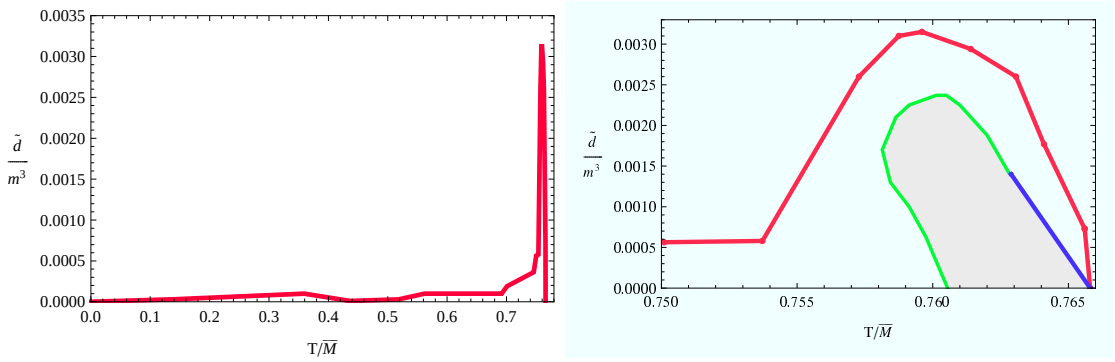

(a) (b)

Figure 8: Charge density at the phase transition in the grand canonical ensemble (red). Figure (b) shows in blue the line of phase transitions identified in the canonical ensemble at fixed n_q [1]. Further the shaded region enclosed by the green and blue curves corresponds to the unstable region identified in [1], in which $(\partial\mu_q/\partial n_q)_T < 0$.

T_{fun}, the critical temperature identified at $n_q = 0$. Here for the grand canonical ensemble with fixed μ_q, we found a first order phase transition extending from $(\mu_q, T) = (0, T_{fun})$ to $(M_q, 0)$, as illustrated in figure 2a. The difference was further highlighted at the end of section 3 with the observation that certain unstable black hole embeddings play a role in describing the phase diagram for the canonical ensemble — the corresponding region is illustrated in figure 8b — but they are not physically relevant for the present analysis of the grand canonical ensemble. These discrepancies pose a paradox since (in the infinite volume limit under consideration here) the canonical and grand canonical ensembles should be equivalent [23].

Before resolving the inconsistency, let us elaborate on what the equivalence stated above entails at a practical level. In the grand canonical ensemble we fix T and μ_q. Minimizing the Gibbs free energy then determines the charge density $n_q = n_q(T, \mu_q)$. In the canonical ensemble, we fix T and n_q and minimize the Helmholtz free energy. This determines the chemical potential $\mu_q = \mu_q(T, n_q)$. However, both of these surfaces, $(T, \mu_q, n_q(T, \mu_q))_{grand}$ and $(T, \mu_q(T, n_q), n_q)_{canon}$, should coincide.[9] That is, a given T and μ_q in the grand canonical ensemble determine a particular value of n_q. Then with this value of n_q and the same temperature T, thermal equilibrium in the canonical ensemble will yield the same value of μ_q as before.

Now the resolution of our inconsistency can be found by examining figure 8 which illustrates the quark density on the black hole embedding along the line of phase transitions in figure 2. Recall that on the other side of the phase transition, the Minkowski embeddings have $n_q = 0$ (or $\tilde{d} = 0$). Hence if we map each configuration in the phase plane in figure 2a to the (n_q, T) plane as in figure 8, we find a gap between the $n_q = 0$ axis and the red curve illustrated in the second figure. Hence we are left to explain how the system accesses these

[9] While this statement is correct for practical purposes, there are, of course, technical subtleties, e.g., at the line of phase transitions where $\partial\mu_q/\partial n_q = 0$. Similar issues arise at $n_q = 0$, where $\partial n_q/\partial\mu_q = 0$ in the low-temperature phase with the present large-λ, large-N_c approximation.

JHEP11(2007)085

values of n_q and T. Here we can use the intuition that we might derive from, say, the liquid to gas transition of ordinary water. That is, we expect that this intermediate regime is filled in by an inhomogeneous mixture where the two phases (with the same chemical potential) coexist. Now the key point, shown in figure 8b, is that the phase transition identified for the canonical ensemble in [1], as well as the region where unstable embeddings were favoured in this ensemble, lies entirely within this intermediate regime where we have just argued that the system should be inhomogeneous. Since the analysis of [1] was restricted to only consider the homogeneous configurations, it misidentified the correct ground state of the system in the small region around the phase transition.

Of course this is not a surprise since, as discussed in [1], the electrical instability of the configurations below the phase transition there already pointed towards an inhomogeneous phase playing a role in the correct phase diagram. The present discussion gives a clearer picture of the nature of this inhomogenous phase and where it is relevant. Let us add that this clarification also highlights a shortcoming of the holographic explorations of the phase diagram of strongly coupled gauge theories here and, for example, in [1, 15 – 17, 28, 35]. That is, they rely on constructing simple and highly symmetric configurations of D-branes and supergravity fields – in particular, configurations describing homogeneous phases of the gauge theory. These symmetries are imposed by hand and, since it is difficult to account for deviations towards less symmetric configurations, the latter are typically ignored. As highlighted by the present discussion, this simplistic approach may fail even in relatively simple circumstances, and so one must be cautious in extracting conclusions based on highly symmetric configurations.

Let us finish with some comments on the possible comparison of the phase diagram obtained here with that of QCD. In addition to the usual caveats at zero density, there are two additional caveats that are particularly relevant at finite chemical potential. The first one is the fact that baryon number in QCD is only carried by fermionic fields, whereas in the type of systems we have studied it is also carried by scalar fields in the fundamental representation. This feature is absent in the D4/D8/$\bar{\text{D}}$8 system of Sakai and Sugimoto [34], whose spectrum in the fundamental representation consists only of fermions. Interesting analyses of this system at finite baryon number chemical potential have recently appeared [35], and further studies will likely be a fruitful avenue for the future. The second caveat is the fact that the very existence of many of the expected phases of QCD at finite chemical potential depend crucially on the fact that $N_c = 3$ (see e.g., [36, 37]). It is therefore unclear to what extent the large-N_c limit may provide a useful approximation at finite chemical potential; some optimistic arguments, however, can be found in [38]. In any case, given the lack of other analytical methods and the difficulties of simulating QCD at finite chemical potential on the lattice, we think it is interesting to explore possible insights coming from the holographic duals of large-N_c gauge theories.

Acknowledgments

It is a pleasure to thank Jorge Casalderrey-Solana, Jaume Gomis, Volker Koch, Jorgen Randrup and Andrei Starinets for useful correspondence and conversations. Research

at the Perimeter Institute is supported in part by funds from NSERC of Canada and MEDT of Ontario. We also acknowledge support from NSF grant PHY-0555669 (DM), an NSERC Discovery grant (RCM), a JSPS Research Fellowship for Young Scientists (SM), an NSERC Canada Graduate Scholarship (RMT) and funding from the Canadian Institute for Advanced Research (RCM,RMT). RCM would also thank the Kavli Institute for Theoretical Physics for hospitality at the beginning of this project. Research at the KITP was supported in part by the NSF under Grant No. PHY05-51164.

References

[1] S. Kobayashi, D. Mateos, S. Matsuura, R.C. Myers and R.M. Thomson, *Holographic phase transitions at finite baryon density*, *JHEP* **02** (2007) 016 [hep-th/0611099].

[2] J.M. Maldacena, *The large-N limit of superconformal field theories and supergravity*, *Adv. Theor. Math. Phys.* **2** (1998) 231 [*Int. J. Theor. Phys.* **38** (1999) 1113] [hep-th/9711200].

[3] O. Aharony, S.S. Gubser, J.M. Maldacena, H. Ooguri and Y. Oz, *Large-N field theories, string theory and gravity*, *Phys. Rept.* **323** (2000) 183 [hep-th/9905111].

[4] E. Witten, *Anti-de Sitter space, thermal phase transition and confinement in gauge theories*, *Adv. Theor. Math. Phys.* **2** (1998) 505 [hep-th/9803131].

[5] J. Babington, J. Erdmenger, N.J. Evans, Z. Guralnik and I. Kirsch, *Chiral symmetry breaking and pions in non-supersymmetric gauge/gravity duals*, *Phys. Rev.* **D 69** (2004) 066007 [hep-th/0306018];
M. Kruczenski, D. Mateos, R.C. Myers and D.J. Winters, *Towards a holographic dual of large-N_c QCD*, *JHEP* **05** (2004) 041 [hep-th/0311270];
I. Kirsch, *Generalizations of the AdS/CFT correspondence*, *Fortschr. Phys.* **52** (2004) 727 [hep-th/0406274].

[6] D. Mateos, R.C. Myers and R.M. Thomson, *Holographic phase transitions with fundamental matter*, *Phys. Rev. Lett.* **97** (2006) 091601 [hep-th/0605046].

[7] D. Mateos, R.C. Myers and R.M. Thomson, *Thermodynamics of the brane*, *JHEP* **05** (2007) 067 [hep-th/0701132].

[8] D. Mateos, R.C. Myers and R.M. Thomson, *Holographic viscosity of fundamental matter*, *Phys. Rev. Lett.* **98** (2007) 101601 [hep-th/0610184].

[9] T. Albash, V.G. Filev, C.V. Johnson and A. Kundu, *A topology-changing phase transition and the dynamics of flavour*, hep-th/0605088;
A. Karch and A. O'Bannon, *Chiral transition of $N = 4$ super Yang-Mills with flavor on a 3-sphere*, *Phys. Rev.* **D 74** (2006) 085033 [hep-th/0605120];
T. Albash, V.G. Filev, C.V. Johnson and A. Kundu, *Global currents, phase transitions and chiral symmetry breaking in large-N_c gauge theory*, hep-th/0605175;
A. Karch and A. O'Bannon, *Metallic AdS/CFT*, *JHEP* **09** (2007) 024 [arXiv:0705.3870];
A. O'Bannon, *Hall conductivity of flavor fields from AdS/CFT*, *Phys. Rev.* **D 76** (2007) 086007 [arXiv:0708.1994].

[10] R.C. Myers, A.O. Starinets and R.M. Thomson, *Holographic spectral functions and diffusion constants for fundamental matter*, arXiv:0706.0162.

[11] C. Hoyos, K. Landsteiner and S. Montero, *Holographic meson melting*, *JHEP* **04** (2007) 031 [hep-th/0612169].

[12] O. Aharony, J. Sonnenschein and S. Yankielowicz, *A holographic model of deconfinement and chiral symmetry restoration*, *Ann. Phys. (NY)* **322** (2007) 1420 [hep-th/0604161];
A. Parnachev and D.A. Sahakyan, *Chiral phase transition from string theory*, *Phys. Rev. Lett.* **97** (2006) 111601 [hep-th/0604173];
Y.-H. Gao, W.-S. Xu and D.-F. Zeng, *NGN, QCD_2 and chiral phase transition from string theory*, *JHEP* **08** (2006) 018 [hep-th/0605138];
K. Peeters, J. Sonnenschein and M. Zamaklar, *Holographic melting and related properties of mesons in a quark gluon plasma*, *Phys. Rev.* **D 74** (2006) 106008 [hep-th/0606195];
E. Antonyan, J.A. Harvey and D. Kutasov, *The Gross-Neveu model from string theory*, *Nucl. Phys.* **B 776** (2007) 93 [hep-th/0608149].

[13] T. Umeda, K. Nomura and H. Matsufuru, *Charmonium at finite temperature in quenched lattice QCD*, *Eur. Phys. J.* **C 39S1** (2005) 9 [hep-lat/0211003];
M. Asakawa and T. Hatsuda, *J/ψ and η/c in the deconfined plasma from lattice QCD*, *Phys. Rev. Lett.* **92** (2004) 012001 [hep-lat/0308034];
S. Datta, F. Karsch, P. Petreczky and I. Wetzorke, *Behavior of charmonium systems after deconfinement*, *Phys. Rev.* **D 69** (2004) 094507 [hep-lat/0312037];
A. Jakovac, P. Petreczky, K. Petrov and A. Velytsky, *On charmonia survival above deconfinement*, hep-lat/0603005;
G. Aarts et al., *Charmonium spectral functions in $N_f = 2$ QCD at high temperature*, PoS(LAT2006)126 [hep-lat/0610065];
G. Aarts, C. Allton, J. Foley, S. Hands and S. Kim, *Spectral functions at non-zero momentum in hot QCD*, PoS(LAT2006)134 [hep-lat/0610061];
P. Petreczky, *Lattice QCD at finite temperature*, *Nucl. Phys.* **A 785** (2007) 10 [hep-lat/0609040];
G. Aarts, C. Allton, J. Foley, S. Hands and S. Kim, *Spectral functions at small energies and the electrical conductivity in hot, quenched lattice QCD*, *Phys. Rev. Lett.* **99** (2007) 022002 [hep-lat/0703008];
H.B. Meyer, *A calculation of the shear viscosity in* SU(3) *gluodynamics*, arXiv:0704.1801;
G. Aarts, C. Allton, M.B. Oktay, M. Peardon and J.-I. Skullerud, *Charmonium at high temperature in two-flavor QCD*, arXiv:0705.2198.

[14] S. Matsuura, *On holographic phase transitions at finite chemical potential*, arXiv:0711.0407.

[15] S. Nakamura, Y. Seo, S.-J. Sin and K.P. Yogendran, *Baryon-charge chemical potential in AdS/CFT*, arXiv:0708.2818.

[16] K. Ghoroku, M. Ishihara and A. Nakamura, *$D3/D7$ holographic gauge theory and chemical potential*, arXiv:0708.3706.

[17] A. Karch and A. O'Bannon, *Holographic thermodynamics at finite baryon density: some exact results*, arXiv:0709.0570.

[18] A. Karch and L. Randall, *Open and closed string interpretation of SUSY CFT's on branes with boundaries*, *JHEP* **06** (2001) 063 [hep-th/0105132];
A. Karch and E. Katz, *Adding flavor to AdS/CFT*, *JHEP* **06** (2002) 043 [hep-th/0205236].

[19] C.P. Herzog, A. Karch, P. Kovtun, C. Kozcaz and L.G. Yaffe, *Energy loss of a heavy quark moving through $N = 4$ supersymmetric Yang-Mills plasma*, *JHEP* **07** (2006) 013 [hep-th/0605158].

[20] I. Racz and R.M. Wald, *Extension of space-times with Killing horizon*, *Class. and Quant. Grav.* **9** (1992) 2643.

JHEP11(2007)085

[21] M. Kruczenski, D. Mateos, R.C. Myers and D.J. Winters, *Meson spectroscopy in AdS/CFT with flavour*, *JHEP* **07** (2003) 049 [hep-th/0304032].

[22] S.W. Hawking, *The path-integral approach to quantum gravity*, in *General relativity: an Einstein centenary survey*, eds. S.W. Hawking and W. Israel, Cambridge University Press, Cambridge U.K. (1979).

[23] See, for example D. Ruelle, *Statistical mechanics: rigorous results*, New York, Benjamin (1969).

[24] A. Karch, A. O'Bannon and K. Skenderis, *Holographic renormalization of probe D-branes in AdS/CFT*, *JHEP* **04** (2006) 015 [hep-th/0512125].

[25] A. Chamblin, R. Emparan, C.V. Johnson and R.C. Myers, *Holography, thermodynamics and fluctuations of charged AdS black holes*, *Phys. Rev.* **D 60** (1999) 104026 [hep-th/9904197]; *Charged AdS black holes and catastrophic holography*, *Phys. Rev.* **D 60** (1999) 064018 [hep-th/9902170].

[26] J. Erdmenger, M. Kaminski and F. Rust, *Isospin diffusion in thermal AdS/CFT with flavor*, *Phys. Rev.* **D 76** (2007) 046001 [arXiv:0704.1290].

[27] D. Mateos and L. Patino, *Bright branes for strongly coupled plasmas*, arXiv:0709.2168.

[28] S. Nakamura, Y. Seo, S.-J. Sin and K.P. Yogendran, *A new phase at finite quark density from AdS/CFT*, hep-th/0611021.

[29] A.W. Peet and J. Polchinski, *UV/IR relations in AdS dynamics*, *Phys. Rev.* **D 59** (1999) 065011 [hep-th/9809022];
R.C. Myers and R.M. Thomson, *Holographic mesons in various dimensions*, *JHEP* **09** (2006) 066 [hep-th/0605017].

[30] E. Witten, *Baryons and branes in anti de Sitter space*, *JHEP* **07** (1998) 006 [hep-th/9805112];
C.G. Callan Jr., A. Guijosa and K.G. Savvidy, *Baryons and string creation from the fivebrane worldvolume action*, *Nucl. Phys.* **B 547** (1999) 127 [hep-th/9810092].

[31] C.G. Callan Jr., A. Guijosa, K.G. Savvidy and O. Tafjord, *Baryons and flux tubes in confining gauge theories from brane actions*, *Nucl. Phys.* **B 555** (1999) 183 [hep-th/9902197].

[32] S. Hong, S. Yoon and M.J. Strassler, *Quarkonium from the fifth dimension*, *JHEP* **04** (2004) 046 [hep-th/0312071].

[33] J.L. Hovdebo, M. Kruczenski, D. Mateos, R.C. Myers and D.J. Winters, *Holographic mesons: adding flavor to the AdS/CFT duality*, *Int. J. Mod. Phys.* **A 20** (2005) 3428.

[34] T. Sakai and S. Sugimoto, *Low energy hadron physics in holographic QCD*, *Prog. Theor. Phys.* **113** (2005) 843 [hep-th/0412141]; *More on a holographic dual of QCD*, *Prog. Theor. Phys.* **114** (2006) 1083 [hep-th/0507073].

[35] K.-Y. Kim, S.-J. Sin and I. Zahed, *Dense hadronic matter in holographic QCD*, hep-th/0608046;
N. Horigome and Y. Tanii, *Holographic chiral phase transition with chemical potential*, *JHEP* **01** (2007) 072 [hep-th/0608198];
A. Parnachev and D.A. Sahakyan, *Photoemission with chemical potential from QCD gravity dual*, *Nucl. Phys.* **B 768** (2007) 177 [hep-th/0610247];

JHEP11(2007)085

D. Yamada, *Sakai-Sugimoto model at high density*, arXiv:0707.0101;
O. Bergman, G. Lifschytz and M. Lippert, *Holographic nuclear physics*, arXiv:0708.0326;
J.L. Davis, M. Gutperle, P. Kraus and I. Sachs, *Stringy NJLS and Gross-Neveu models at finite density and temperature*, *JHEP* **10** (2007) 049 [arXiv:0708.0589];
M. Rozali, H.-H. Shieh, M. Van Raamsdonk and J. Wu, *Cold nuclear matter in holographic QCD*, arXiv:0708.1322;
K.-Y. Kim, S.-J. Sin and I. Zahed, *The chiral model of Sakai-Sugimoto at finite baryon density*, arXiv:0708.1469.

[36] K. Rajagopal and F. Wilczek, *The condensed matter physics of QCD*, hep-ph/0011333.

[37] M.A. Stephanov, *QCD phase diagram: an overview*, PoS(LAT2006)024 [hep-lat/0701002].

[38] L. McLerran and R.D. Pisarski, *Phases of cold, dense quarks at large-N_c*, *Nucl. Phys.* **A 796** (2007) 83 [arXiv:0706.2191].

JHEP11(2007)085